Effect of Porphyrin Ligands on the Regioselective Dehydrogenation versus Epoxidation of Olefins by Oxoiron(IV) Mimics of Cytochrome P450†

Devesh Kumar,*,‡ Laleh Tahsini,§ Sam P. de Visser,*,§ Hye Yeon Kang,|| Soo Jeong Kim,|| and Wonwoo Nam*,||

Contribution from Molecular Modeling Group, Indian Institute of Chemical Technology, Hyderabad 500-607, India, The Manchester Interdisciplinary Biocenter and the School of Chemical Engineering and Analytical Science, The University of Manchester, 131 Princess Street, Manchester M1 7DN, United Kingdom, and Department of Chemistry and Nano Science, Department of Bioinspired Science, Centre for Biomimetic Systems, Ewha Womans University, Seoul 120-750, Korea

Received: March 30, 2009; Revised Manuscript Received: June 29, 2009

The cytochromes P450 are versatile enzymes involved in various catalytic oxidation reactions, such as hydroxylation, epoxidation and dehydrogenation. In this work, we present combined experimental and theoretical studies on the change of regioselectivity in cyclohexadiene oxidation (i.e., epoxidation vs dehydrogenation) by oxoiron(IV) porphyrin complexes bearing different porphyrin ligands. Our experimental results show that meso-substitution of the porphyrin ring with electron-withdrawing substituents leads to a regioselectivity switch from dehydrogenation to epoxidation, affording the formation of epoxide as a major product. In contrast, electron-rich iron porphyrins are shown to produce benzene resulting from the dehydrogenation of cyclohexadiene. Density functional theory (DFT) calculations on the regioselectivity switch of epoxidation vs dehydrogenation have been performed using three oxoiron(IV) porphyrin oxidants with hydrogen atoms, phenyl groups, and pentachlorophenyl ($ArCl_5$) groups on the meso-position. The DFT studies show that the epoxidation reaction by the latter catalyst is stabilized because of favorable interactions of the substrate with halogen atoms of the meso-ligand as well as with pyrrole nitrogen atoms of the porphyrin macrocycle. Hydrogen abstraction transition states, in contrast, have a substrate-binding orientation further away from the porphyrin pyrrole nitrogens, and they are much less stabilized. Finally, the regioselectivity of dehydrogenation versus hydroxylation is rationalized using thermodynamic cycles.

Introduction

Cytochromes P450 (P450) are oxygen-activating enzymes involved in key processes in biosystems ranging from drug metabolism, to the biosynthesis of hormones, to the detoxification processes in the liver.[1,2] Figure 1 shows an extract of the active site of a typical P450 enzyme, namely, $P450_{cam}$,[3] which is a bacterial P450 that regioselectively hydroxylates camphor at the C^5 position.[4] The enzyme active site is a heme group with a metal (iron) embedded in its center and that is linked to the protein via a sulfur bridge of a cysteinate residue (Cys_{357} in $P450_{cam}$).[5] The active center binds molecular oxygen, which is converted into an oxoiron(IV) active species, Compound I (Cpd I), via a series of reduction and protonation steps. Cpd I, however, is elusive, but kinetic isotope effects and product distributions implicate it to be involved in substrate monooxygenation reactions.[6]

P450 enzymes catalyze a range of different reaction mechanisms; for instance, aliphatic C−H hydroxylation, aromatic C−H hydroxylation, C═C double bond epoxidation, sulfoxidation, *N*-dealkylation, and dehydrogenation.[2] As a consequence, some substrates react at the active center of P450 enzymes to give competing reaction mechanisms leading to one or more different products. Mutagenesis studies, whereby key active site residues are replaced, occasionally give a regioselectivity switch from one product to another. Furthermore, it has been shown that a regioselectivity switch can also occur through the replacement of hydrogen atoms in the substrate by deuterium atoms, which is termed metabolic switching.[7] In particular, hydroxylation took place at the C^3 position with deuterated 5,6-*exo*-*exo*-norcamphor at the C^5 and C^6 positions, whereas in the nondeuterated substrate, the C^5 position was activated. Similar regioselectivity switches were observed for toluene hydroxylation by P450 enzymes.[8]

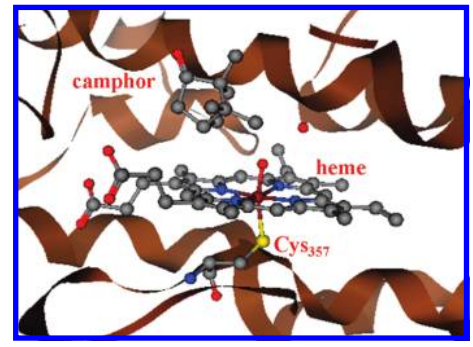

Figure 1. Extract of the active site of $P450_{cam}$ as taken from the 1DZ9 pdb file with substrate (camphor), heme, and its axial ligand (Cys_{357}) highlighted.

These subtle changes in regioselectivity preference by P450 enzymes have triggered many studies to try to establish factors that drive reaction mechanisms. In biomimetic studies, it was

† Part of the "Walter Thiel Festschrift".

* Corresponding authors. E-mail: dkclcre@yahoo.com (D.K.); sam.devisser@manchester.ac.uk (S.P.d.V.); wwnam@ewha.ac.kr (W.N.).
‡ Indian Institute of Chemical Technology.
§ The University of Manchester.
|| Ewha Womans University.

10.1021/jp9028694 CCC: $40.75
Published on Web 08/06/2009

shown that the meso-substituent on the porphyrin ring influences the oxidative power of the oxoiron(IV) oxidant.[9] In particular, electron-deficient iron(III) porphyrins afforded a much higher yield of epoxide products in comparison with oxidants with fewer electron-deficient substituents.[10] Moreover, studies on a series of metal−oxo porphyrin complexes with electron-withdrawing meso-substituents showed a strong ^{17}O NMR shift to higher frequencies that correlated linearly with the force constant of the metal−oxo bond as well as with the rate constant of triphenylphosphine oxidation, which implicates a direct correlation between meso-substitution and the strength of the Fe−O bond of the oxidant.[11] However, the exact nature of the meso-substituent and its influence on the reaction mechanisms has never been studied in depth. To gain insight into the meso-substituent effect on the electronic and catalytic properties of the oxoiron(IV) center, we have performed combined experimental and theoretical studies on cyclohexadiene (CHD) activation by oxoiron(IV) porphyrin oxidants with variable substituents on the meso-position. Earlier studies of us and others have established procedures to generate oxoiron(IV) porphyrin cation radical species using single oxygen atom donors such as iodosylbenzene (PhIO) and *m*-chloroperbenzoic acid (*m*-CPBA). These oxoiron(IV) porphyrin complexes have been shown to react readily with aliphatic groups by hydrogen atom abstraction and with C=C double bonds to give epoxide products.[12] As such, CHD reacts with Cpd I to form epoxide products or alternatively lead to dehydrogenation to form benzene.[13] The studies presented in this work show that a substituent on the meso-position changes the electronic properties of the porphyrin ring leading to subtle differences in electron affinities of the oxidant. Moreover, bulky groups on the meso-position influence substrate binding processes and access to the oxoiron(IV) group.

Methods

Experimental Section. Commercially available reagents were of the best available purity and were used without further purification unless otherwise noted. Acetonitrile (CH_3CN) and dichloromethane (CH_2Cl_2) were dried according to literature procedures and distilled under Argon prior to use.[13] *m*-CPBA was purified by washing with phosphate buffer (pH 7.4) first, followed by water and then dried under reduced pressure.[14] PhIO was prepared by a literature method.[15] Fe(TPFPP)Cl (TPFPP = *meso*-tetrakis(pentafluorophenyl)porphyrin) was purchased from Aldrich Chemical Co., whereas Fe(TMP)Cl (TMP = *meso*-tetramesitylporphyrin) and Fe(TDCPP)Cl (TDCPP = *meso*-tetrakis(2,6-dichlorophenyl)porphyrin) were obtained from Frontier Scientific Inc. (Logan, UT). Fe(TF4TMAP)$(CF_3SO_3)_5$ (TF4TMAP = *meso*-tetrakis(2,3,5,6-tetrafluoro-4-*N*,*N*,*N*-trimethylaniliniumyl)porphyrin) was synthesized using commonly known procedures.[16] Figure 2 shows geometries and labels of the various substituted porphyrin macrocycles at the meso-position studied in this work.

Oxidant (0.10 mmol), either PhIO or *m*-CPBA, was added to a reaction solution containing iron(III) porphyrin chloride (2 mM) and 1,4-cyclohexadiene (0.10 mmol) in a solvent mixture (2 mL) of CH_3CN and CH_2Cl_2 (3:1) at 25 °C. After stirring for 10 min and filtering through an 0.45 μM filter, the reaction mixture was analyzed with Agilent Technologies 6890N gas chromatography equipped with a FID detector (GC) and Thermo Finnigan (Austin, TX) FOCUS DSQ (dual stage quadrupole) mass spectrometer interfaced with a Finnigan FOCUS gas chromatograph (GC-MS). We identified products by comparing retention times and mass patterns with those of known authentic samples. We determined product yields by comparison against

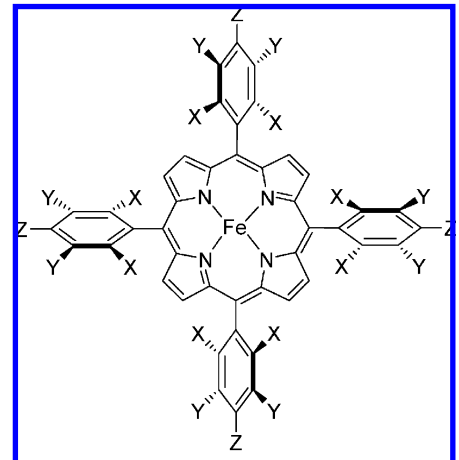

	X	Y	Z
TPP:	H	H	H
TMP:	Me	H	Me
TDCPP:	Cl	H	H
TPFPP:	F	F	F
TPCPP:	Cl	Cl	Cl
TF4TMAP:	F	F	TMA

Figure 2. Definition of the oxidants studied in this work. TMA stands for trimethylaniliniumyl.

standard curves prepared with authentic samples and by using *n*-decane as an internal standard.

Density Functional Theory Calculations. The calculations presented in this work were all obtained from density functional theory (DFT) calculations on biomimetic oxoiron(IV) porphyrin complexes using previously described procedures.[17] Our model is iron−protoporphyrin IX, whereby all side chains of the porphyrin were initially abbreviated with hydrogen atoms (Por). The active species (Cpd I) is an oxoiron(IV) porphyrin cation radical system with a chloride axial ligand similar to that of previous studies of ours in the field: $[Fe^{IV}{=}O(Por^{+\bullet})Cl]$.[18] We studied the regioselective epoxidation and dehydrogenation of 1,3-cyclohexadiene and 1,4-cyclohexadiene as model substrates using DFT with the unrestricted B3LYP method[19] because earlier work of ours on related systems predicted rate constants and kinetic isotope effects in good agreement with experiment.[20] Initial geometry optimizations employed a modest double-ζ quality LACVP basis set on iron and 6-31G on the rest of the atoms (basis set B1).[21] All structures were subjected to a full geometry optimization in Gaussian-03, followed by an analytical frequency calculation.[22] Subsequent, single-point calculations on the optimized geometries with a triple-ζ LACV3P+ basis set on iron and 6-311+G* on the rest of the atoms were done in Jaguar 7.0 to improve the energetics (basis set B2).[23] Local minima described here had real frequencies only, whereas the transition states were characterized by a single imaginary frequency for the correct mode. All charges reported in this work were taken from the atomic polar tensor (APT) charges from the Gaussian frequency calculations. The effect of the environment was tested via single-point calculations at B3LYP/B1 in Jaguar in a continuum solvent with a dielectric constant of ε = 5.7 and a probe radius of 2.72 Å.

In a second set of calculations, we studied the effect of meso-substitution on the electronic and catalytic properties of the oxoiron(IV) species. First, we studied the electronic properties of doublet and quartet oxoiron(IV) species with phenyl, pen-

SCHEME 1

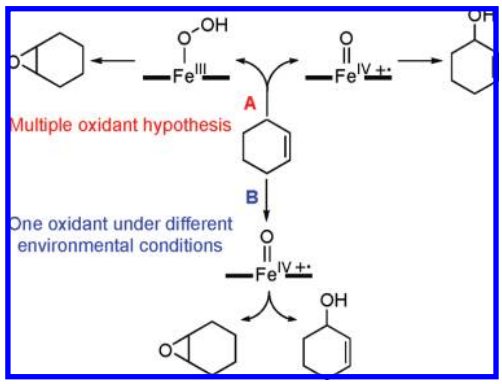

tachlorophenyl ($ArCl_5$), and methoxy substituents on the four meso-positions to give *meso*-tetraphenylporphyrin (TPP), *meso*-tetrakis(pentachlorophenyl)porphyrin (TPCPP), and *meso*-tetramethoxyporphyrin. In addition, using Fe^{IV}=O($TPP^{+\bullet}$)Cl and Fe^{IV}=O($TPCPP^{+\bullet}$)Cl, we re-evaluated the reaction mechanisms for epoxidation and dehydrogenation of 1,3-cyclohexadiene using Jaguar. Full optimizations were done in Jaguar with basis set B1, followed by single-point calculations with basis set B2 in the gas phase and in a continuum solvent with dielectric constant of $\varepsilon = 5.7$. Because of the size of these systems, we only ran frequency calculations on the optimized geometries for the mechanism using Fe^{IV}=O($TPP^{+\bullet}$)Cl as an oxidant and the transition-state structures ^{4}**TS**$_H$(TPCPP) and ^{4}**TS**$_E$(TPCPP).

To test the effect of the density functional method on the relative energies, we ran single-point calculations with the OPBE and PW91B95 density functional methods for the reaction mechanism of $^{4,2}Fe^{IV}$=O($Por^{+\bullet}$)Cl with 1,3-cyclohexadiene.[24,25] The trends are reproduced with alternative density functionals (Supporting Information) so that we do not expect major changes because of the choice of the density functional method.

Results and Discussion

Dehydrogenation versus Epoxidation in Iron Porphyrin-Catalyzed Oxidation Reactions. It has been shown in enzymatic and biomimetic reactions that products formed in the epoxidation of olefins are different depending on reaction conditions.[26−31] For example, Coon and coworkers examined the effect of site-directed mutagenesis of threonine to alanine on the epoxidation of olefins with cytochromes P450 and their mutants and observed the regioselectivity change from epoxide formation to allylic oxidation.[27] The authors proposed that the formation of different products in the reactions of cytochromes P450 and their mutants was due to the involvement of two different active oxidants with electrophilic properties in the oxidation of cyclohexene, such as a ferric−hydroperoxo and an iron(IV)−oxo porphyrin π-cation radical for the epoxidation and allylic hydroxylation, respectively (Scheme 1, pathway A).[27] Contrary to the proposal derived from enzymatic studies, Groves and coworkers have shown in biomimetic studies that the epoxidation of cyclohexene by $[Fe^{III}(TMP)]^+$ and oxidants such as *m*-CPBA and PhIO yielded products derived from both epoxidation (e.g., cyclohexene oxide) and allylic hydroxylation (e.g., cyclohexen-3-ol and cyclohexen-3-one) and that the amounts of epoxidation and allylic hydroxylation products changed significantly depending on reaction temperatures, choice of the selected oxidants, and axial ligands of the iron porphyrin catalyst.[28] Nam and coworkers supported the assertion of Groves and coworkers by showing that the regioselectivity of C=C epoxidation versus allylic C−H hydroxylation in the oxygenation of olefins by in situ-generated oxoiron(IV) porphyrin π-cation radicals depends significantly on the reaction conditions such as reaction temperature, the electronic nature of iron porphyrins, and substrates.[29] These results demonstrated that the regioselectivity of C=C epoxidation versus C−H hydroxylation in the oxygenation of cyclohexene by a single oxidant, ($TMP^{+\bullet}$)Fe^{IV}=O(X), can be altered depending on the reaction conditions (Scheme 1B). The results further suggest that the regioselectivity change does not implicate the participation of two distinct intermediates in olefin oxidations. Very recently, Fujii and coworkers interpreted the change of the regioselectivity with that where the epoxidation reaction is enthalpy-controlled, whereas the allylic hydroxylation reaction is entropy-controlled.[30] In the present study, we extended the study of the porphyrin ligand effect on the regioselectivity change to elucidate the origin of the regioselectivity change depending on the reaction conditions and the substituent effect of the porphyrin ligand.

SCHEME 2

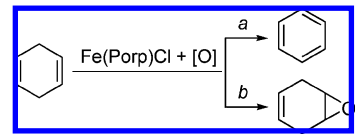

TABLE 1: Oxidation of 1,4-Cyclohexadiene by Iron(III) Porphyrin Complexes and Oxidants[a]

			products (%)[b,c]	
entry	catalyst	oxidant	benzene	4-cyclohexadiene oxide
1	Fe(TMP)Cl	PhIO	37 ± 4	2 ± 1
		m-CPBA	34 ± 4	3 ± 1
2	Fe(TDCPP)Cl	PhIO	14 ± 3	27 ± 3
		m-CPBA	17 ± 3	29 ± 3
3	Fe(TPFPP)Cl	PhIO	<1	32 ± 3
		m-CPBA	<1	30 ± 3
4	Fe(TF4TMAP)$(CF_3SO_3)_5$	PhIO	<1	35 ± 3
		m-CPBA	<1	32 ± 3

[a] See Experimental Section for detailed reaction conditions. [b] Yields (%) are calculated on the basis of the amounts of oxidant added. [c] Product distributions did not change depending on reaction temperatures (e.g., at −20 °C).

The regioselectivity of dehydrogenation versus epoxidation in the oxidation of olefins by iron(III) porphyrin complexes and oxidants was examined using 1,4-cyclohexadiene (CHD) as a substrate. The oxidation of CHD by PhIO or *m*-CPBA catalyzed by an iron(III) porphyrin complex afforded the formation of benzene and 4-cyclohexadiene oxide (Scheme 2) depending on the electron-richness of porphyrin ligands. The results shown in Table 1 show that Fe(TMP)Cl, which is an electron-rich iron(III) porphyrin catalyst, yielded benzene as the major product with the formation of a trace amount of epoxide product (entry 1). In contrast, 4-cyclohexadiene oxide was the major product in the reactions of electron-deficient iron porphyrin complexes, such as Fe(TPFPP)Cl and Fe(TF4TMAP)$(CF_3SO_3)_5$ (entries 3 and 4). We have also observed the formation of benzene and 4-cyclohexadiene oxide in the reaction of Fe(TDCPP)Cl (entry 2); the electron-richness of this iron porphyrin complex was between the electron-rich and -deficient iron porphyrins. These results indicate that electron-rich iron porphyrins prefer C−H bond activation to give olefin dehydrogenation (Scheme 2, pathway a), whereas oxygen atom transfer to a double bond is the preferred pathway in the reaction of electron-deficient iron porphyrin catalysts (Scheme 2, pathway b).[9,31] Furthermore, the product distributions were identical irrespective of oxidants,

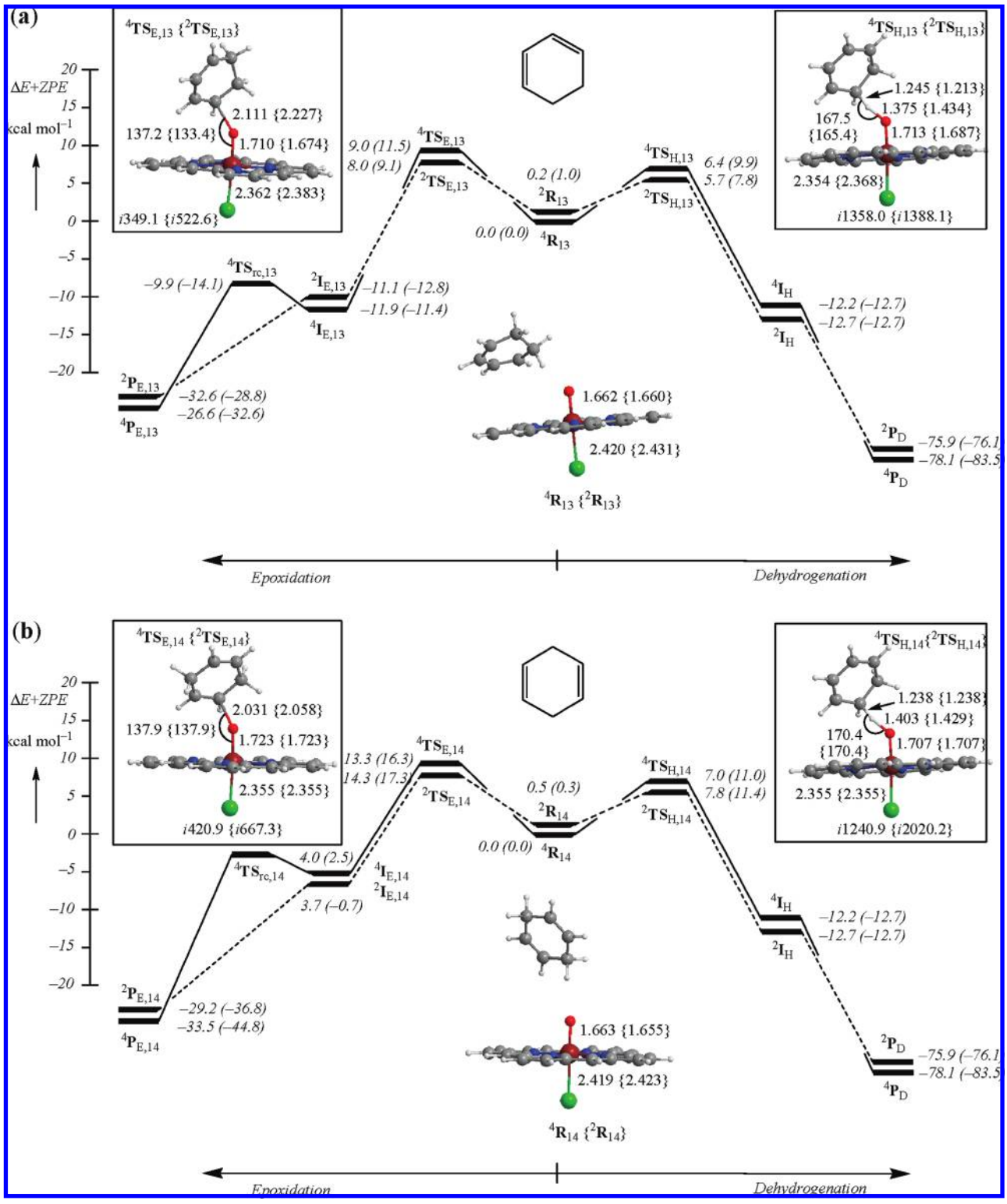

Figure 3. Potential energy profiles of (a) 1,3-cyclohexadiene and (b) 1,4-cyclohexadiene epoxidation and dehydrogenation by ^{4,2}**R**, as calculated with UB3LYP. Energies contain ZPE and are obtained with basis set B1, whereas values in parentheses were calculated with basis set B2 and include solvent corrections. Also given are geometries of the reactants and rate-determining transition states with bond lengths in angstroms, angles in degrees, and the value of the imaginary frequency in wavenumbers.

suggesting that a common intermediate (for example, a high-valent iron(IV)−oxo porphyrin π-cation radical species) was generated as reactive species responsible for the dehydrogenation and epoxidation reactions.[32]

Theoretical Modeling of the Reaction Mechanism. Because our experimental studies on the reaction of oxoiron(IV) porphyrins with 1,4-cyclohexadiene (CHD) show that a mixture of dehydrogenation and epoxidation products are formed depending on the nature of the group on the meso-position (Table 1), we decided to do a series of DFT calculations to trace the origins of this regioselectivity switch. Let us first start with a description of the simplest chemical system, whereby the porphyrin ring (Por) has no side chains and the reaction of the oxoiron(IV) species is with CHD, that is, Fe^{IV}═O($Por^{+\bullet}$)-

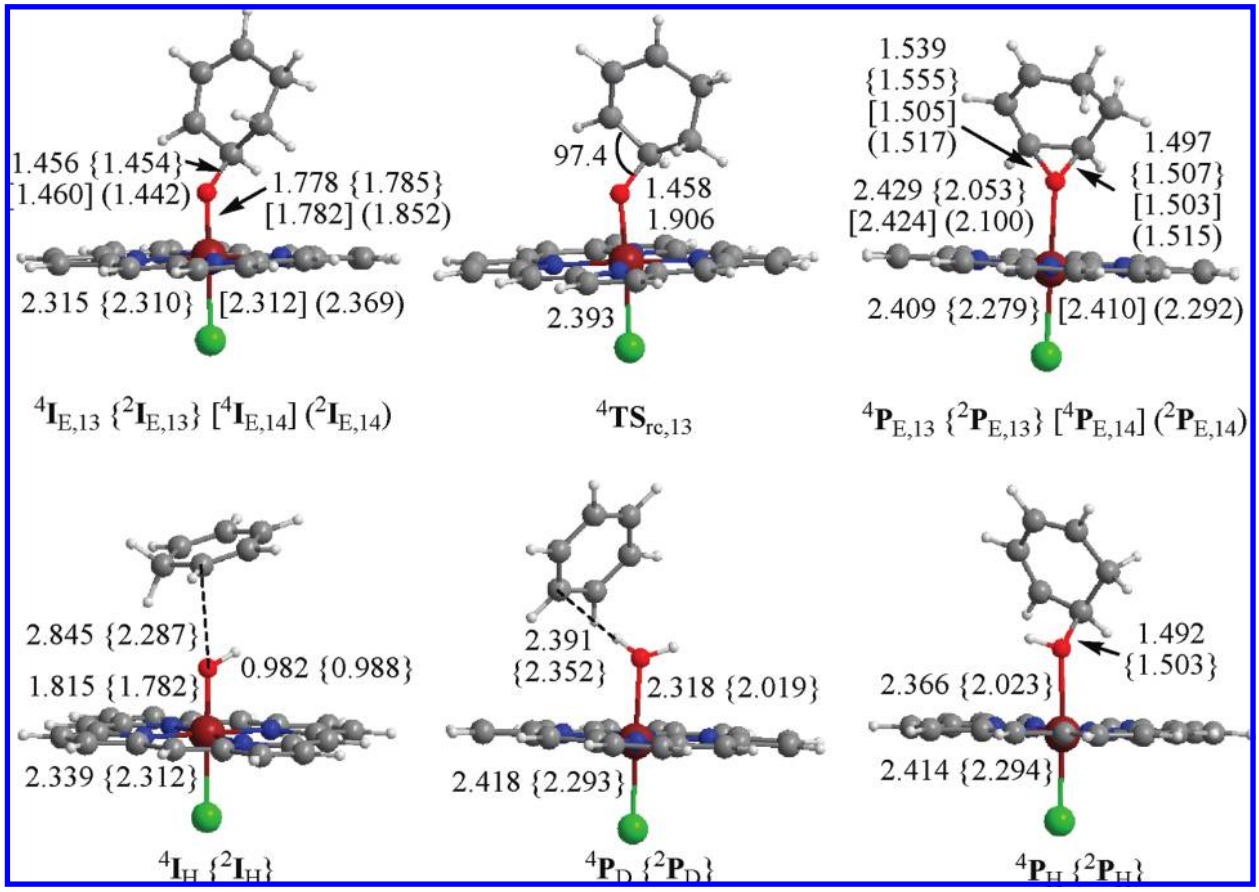

Figure 4. Optimized geometries of critical points along the reaction coordinates shown in Figure 3. All structures optimized with UB3LYP/B1 with bond lengths given in angstroms and angles in degrees.

$Cl-C_6H_8$. Figure 3 shows the potential energy profile of 1,3-cyclohexadiene and 1,4-cyclohexadiene epoxidation and dehydrogenation by $[Fe^{IV}{=}O(Por^{+\bullet})Cl]$ (designated **R**) on the doublet and quartet spin-state surfaces as calculated with DFT.

The reactions are stepwise starting from the degenerate spin states of Cpd I, doublet (^{2}**R**) and quartet (^{4}**R**). As shown before, Cpd I has close-lying doublet and quartet spin states with the same orbital occupation, that is, $\pi^*_{xz}{}^1\ \pi^*_{yz}{}^1\ a_{2u}{}^1$, leading to an electronic configuration of $[Fe^{IV}{=}O(Por^{+\bullet})Cl]$.[33] The π^* set of orbitals are antibonding orbitals for the Fe−O interaction through atomic orbital interactions between the $3d_{xz,yz}$ on iron and $2p_{x,y}$ on oxygen. The third unpaired electron is on a heme-type orbital that has an a_{2u} label in D_{4h} symmetry.[34] Because the interactions of the $\pi^*_{xz,yz}$, on one hand, with a_{2u}, on the other hand, are small, the three unpaired electrons can be ferromagnetically coupled into an overall quartet spin state or antiferromagnetically coupled into a doublet spin state. It has been shown that in oxoiron(IV) species of heme enzymes these two states are close in energy and environmental perturbations and the nature of the axial ligand determine the ordering and relative energy of the two spin states.[35] As a consequence, Cpd I reacts with substrates via two-state-reactivity patterns on competing doublet and quartet spin state surfaces.[36]

The reaction in Figure 3 starts from the center with ^{2,4}**R**. Whereas the mechanism to the left leads to epoxide products, the mechanism to the right affords dehydrogenation products. The epoxidation reaction passes a C−O bond activation barrier (^{4,2}**TS**$_E$) to form a radical intermediate (^{4,2}**I**$_E$), followed by a ring-closure barrier (^{4,2}**TS**$_{rc}$) to give epoxide products. This mechanism is similar to the one that we and others observed before for alkene epoxidation by Cpd I of P450.[37] The barrier ^{4,2}**TS**$_E$ is the rate-determining step in the reaction mechanism, and only on the quartet spin-state surface was a significant ring-closure barrier found. On the doublet spin-state surface, the ring-closure barrier was found to be negligible, similar to radical rebound studies of alkane hydroxylation reactions.[38] Optimized geometries of ^{4,2}**TS**$_E$ are characteristic of epoxidation transition states with long C−O bonds and an imaginary frequency representing a C−O stretch vibration. Optimized geometries for epoxidation of 1,3-cyclohexadiene and 1,4-cyclohexadiene are very similar, and the only differences are related to the relative energies. Because of more π-system stabilization of the radical intermediates, ^{4,2}**I**$_{E,13}$ are significantly lower in energy than ^{4,2}**I**$_{E,14}$, and so are the epoxidation barriers. Optimized geometries of subsequent structures in the epoxidation mechanism (^{4,2}**I**$_E$, ^{4}**TS**$_{rc}$, and ^{4,2}**P**$_E$) are shown in Figure 4. These structures show typical features of epoxidation intermediate, ring-closure transition state, and product complexes and resemble geometries of substrate epoxidation of smaller molecules previously published.[37]

The dehydrogenation mechanism proceeds from the center in Figure 3 starting with ^{2,4}**R** by a hydrogen abstraction transition state (^{4,2}**TS**$_H$) that leads to a hydroxo−iron(IV) complex, ^{4,2}**I**$_H$. In a subsequent step, a second hydrogen atom is abstracted to give benzene (i.e., a dehydrogenated product, ^{4,2}**P**$_D$). Note that the mechanisms for hydrogen abstraction by both 1,3-cyclohexadiene and 1,4-cyclohexadiene give the same hydroxo−iron(IV) complex (^{4,2}**I**$_H$), and as a consequence, the rebound/second hydrogen abstraction mechanisms are also the same. Accordingly, the relative energies of the hydrogen abstraction transition states for 1,3-cyclohexadiene and 1,4-cyclohexadiene are within a few kilocalories per mole. In contrast, the epoxidation barriers for 1,3-cyclohexadiene and 1,4-cyclohexa-

diene are much wider apart; therefore, Fe^{IV}=O($Por^{+\bullet}$)Cl will react with 1,4-cyclohexadiene via exclusive dehydrogenation, whereas with 1,3-cyclohexadiene, minor epoxidation products may be formed.

Extensive geometry scans show that the second hydrogen abstraction from $^{4,2}\mathbf{I}_H$ is essentially barrierless on both spin-state surfaces. Alternatively, the hydroxo group can rebound to the radical rest group to form alcohol products ($^{4,2}\mathbf{P}_H$); however, geometry scans for the radical rebound show it to proceed by a much larger barrier than substrate dehydrogenation so that the reaction will generate dehydrogenation rather than hydroxylation products. Later in this work, we will give a thermodynamic explanation for the preference of dehydrogenation over hydroxylation using this substrate. The hydrogen abstraction barriers for 1,3-cyclohexadiene are favored over epoxidation by 2.3 (2.6) kcal mol^{-1} for the doublet (quartet) spin states with a small basis set, whereas improvement of the basis set and solvent corrections decreases these gaps to 1.3 (1.6) kcal mol^{-1}. Although the energy differences are small, they support the experimental studies discussed above, where electron-donating substituents on the meso-position give dehydrogenation products rather than epoxidation products.

Hydrogen abstraction leads to electron transfer into the a_{2u} orbital to generate an iron(IV)−hydroxo complex with orbital occupation of $\pi^*_{xz}{}^1\ \pi^*_{yz}{}^1\ a_{2u}{}^2\ \phi_{Alk}{}^1$, whereby the latter orbital represents the substrate radical. The intermediate complex in the dehydrogenation mechanism, therefore, is an Fe^{IV}(OH)(Por)Cl···$Alk^\bullet$ system with $Alk^\bullet$ as the substrate radical rest group. This is similar to earlier studies of substrate hydroxylation by P450 models, whereby the hydrogen abstraction reaction proceeds with electron transfer from the substrate into the a_{2u} orbital.[39] Optimized geometries show features characteristic of this mechanism with bond lengths in good agreement with the literature. In the hydrogen abstraction transition states ($^{4,2}\mathbf{TS}_{H,13}$ and $^{4,2}\mathbf{TS}_{H,14}$), the transferrable hydrogen atom is slightly closer to the donor-carbon atom than to the acceptor-oxygen atom; for example, r_{CH} = 1.245 (1.213) Å and r_{OH} = 1.375 (1.434) Å for $^4\mathbf{TS}_{H,13}$ ($^2\mathbf{TS}_{H,13}$), respectively, which indicates that the transition-state structures are reactantlike. These transition states are characterized by a large imaginary frequency of *i*1358.0 (*i*1388.1) cm^{-1} for $^4\mathbf{TS}_{H,13}$ ($^2\mathbf{TS}_{H,13}$) and *i*1240.9 (*i*2020.2) cm^{-1} for $^4\mathbf{TS}_{H,14}$ ($^2\mathbf{TS}_{H,14}$), implying that an elevated kinetic isotope effect may be expected upon replacement of the transferrable hydrogen atom with deuterium. After hydrogen abstraction and the formation of the radical intermediate, there are two possible mechanisms to product formation, namely, radical rebound to the hydroxo group to form alcohol products or a second hydrogen abstraction to give benzene and water products (dehydrogenation). Geometrically, the dehydrogenation product is a water molecule interacting with benzene and is essentially a resting state system with an interacting substrate. The structure resembles that of an azole molecule bound to a resting state structure of P450.[40]

Subsequently, we extended our chemical system with either four phenyl or four pentachlorophenyl ($ArCl_5$) groups on the meso-positions of the porphyrin macrocycle to create Cpd I(TPP) and Cpd I(TPCPP) and re-evaluated the epoxidation and dehydrogenation reactions. Before describing these results, let us first make a comparison of Cpd I with three meso-substituted porphyrins in Figure 5, whereby Cpd I(OMe) contains four methoxy groups on the meso-positions. Geometrically, ^{4,2}Cpd I and the meso-substituted structures are almost identical with differences in bond lengths well below 0.01 Å. The Fe−O stretch vibration (ν_{FeO}) of ^{4}Cpd I shifts from 848 to 840 cm^{-1} upon the addition of $ArCl_5$ substituents to the meso-position, which implies that a small change on the strength of the Fe−O bond is incurred. A similar pattern is observed for the group spin densities, where only minor differences are found. Therefore, an extra group on the meso-position does not alter the orbital levels and electronic ground state of Cpd I. The group charges, by contrast, show somewhat larger variations between the different Cpd I structures: The overall charge (Q) on the porphyrin ring decreases from Q_{Por} = 0.21 (0.20) in the unsubstituted system ^{4}Cpd I (^{2}Cpd I) to Q_{Por} = 0.09 (0.10) for ^{4}Cpd I(TPCPP) (^{2}Cpd I(TPCPP)). This decrease in the total charge of the porphyrin ring is mainly due to a decreased charge on the *meso*-carbon atoms to an average from $Q_{C\text{-}meso}$ = 0.40 (0.41) in ^{4}Cpd I (^{2}Cpd I) to 0.67 (0.68) for ^{4}Cpd I(TPCPP) (^{2}Cpd I(TPCPP)). A substituent on the meso-position also has an effect on the charge of the oxygen atom, although the difference is not as dramatic in comparison with the *meso*-carbon atom, but it will influence the electron affinity of the oxidant and its ability to transfer the oxygen atom to substrates. Indeed, a calculation of the one-electron reduced form of these Cpd I complexes, that is, ^{3}Cpd II and ^{3}Cpd II(TPCPP), reveals that the electron affinity (EA) has increased from 3.09 to 4.02 eV for the large system.

Finally, we calculated some key structures in the epoxidation and dehydrogenation reaction mechanisms of 1,3-cyclohexadiene activation by ^{4,2}Cpd I(TPCPP), and the results are given in Figure 6. The mechanisms are similar to those shown above in Figure 3, and so is the labeling of the structures. Because of the size of the chemical system, geometry scans and transition state searches for the hydrogen abstraction and C−O activation in the epoxidation reactions were run only for the quartet spin state. We do not expect dramatic changes for the doublet spin state because the same electron transfer processes occur there. In general, doublet and quartet aliphatic hydrogen abstraction barriers are within a few kilocalories per mole and so are epoxidation barriers.[37,39] Intermediates were calculated for both spin-state structures, although attempts to calculate the iron(IV)−hydroxo complex in the doublet spin state failed and converged to the dehydrogenation product complex instead ($^2\mathbf{P}_D$(TPCPP)).

The potential energy profile shown in Figure 6 predicts dominant epoxidation over hydroxylation by 4.9 kcal mol^{-1} in the gas phase. This regioselectivity is in agreement with the data shown in Table 1, where a switch from dehydrogenation to epoxidation is observed through the addition of electron-withdrawing groups to the meso-position. Because of the size of the chemical system, we ran frequency calculations on only the transition-state geometries of Figure 6. With zero-point energy corrections included, barriers of $^4\mathbf{TS}_E$ = 6.4 kcal mol^{-1} and $^4\mathbf{TS}_H$ = 7.4 kcal mol^{-1} are obtained at the ΔE_{B2} + ZPE_{B1} level of theory, whereas corrections to a dielectric constant change these barriers to 6.8 and 6.9 kcal mol^{-1}, respectively. Therefore, ZPE corrections bring $^4\mathbf{TS}_E$(TPCPP) and $^4\mathbf{TS}_H$(TPCPP) in a dielectric constant within 1 kcal mol^{-1} of each other. These values are in perfect agreement with the product ratios observed for the reaction of Fe=O(TDCPP)Cl with cyclohexadiene (entry 2 in Table 1). Energetically, the epoxidation mechanism shows close similarities to the small model complex depicted in Figure 3 with a slightly lower epoxidation barrier of 7.2 kcal mol^{-1}, whereas the hydrogen abstraction barrier is considerably destabilized with basis set B1.

In addition, we calculated the intermediate complexes in the reaction mechanism ($^{4,2}\mathbf{I}_E$ and $^{4,2}\mathbf{I}_H$) for the reaction of $^{4,2}Fe^{IV}$=O($TPP^{+\bullet}$)Cl with 1,3-cyclohexadiene. At the ΔE_{B2} +

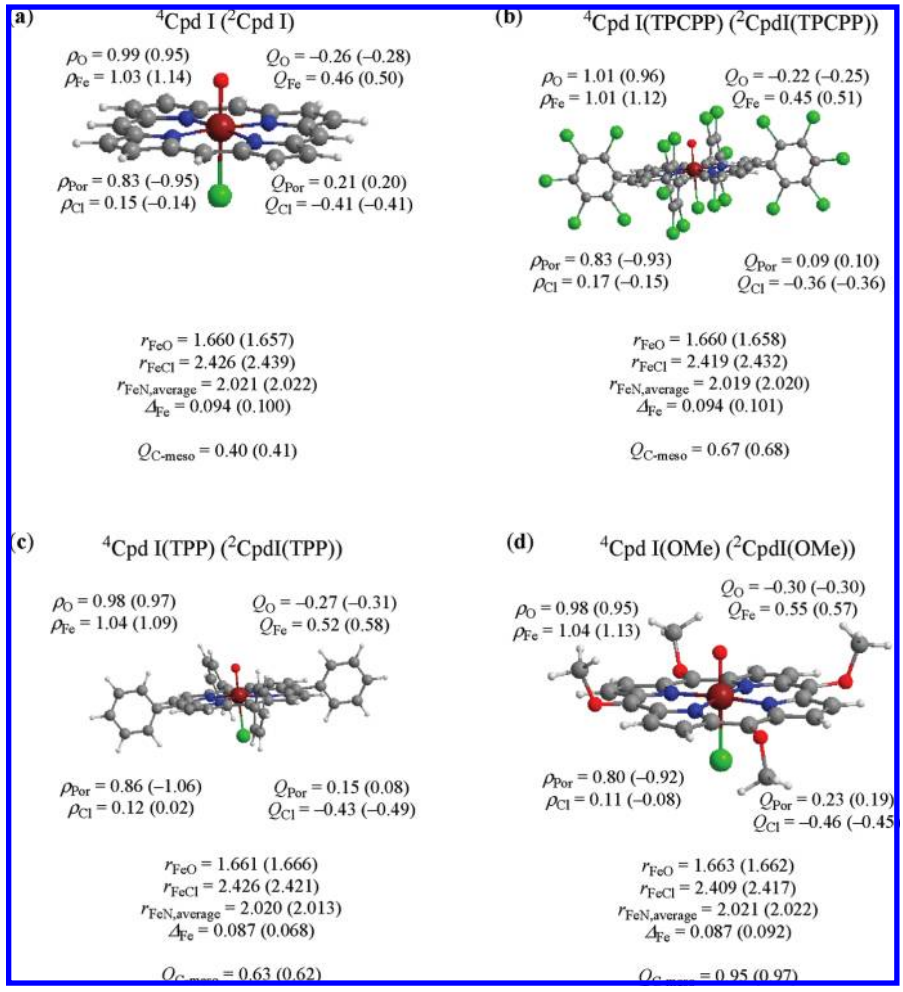

Figure 5. Optimized geometries, group charges (Q), and group spin densities (ρ) of ^{4,2}Cpd I, ^{4,2}Cpd I(TPCPP), ^{4,2}Cpd I(TPP), and ^{4,2}Cpd I(OMe) with bond lengths in angstroms. The $r_{FeN,average}$ distance is the average Fe−N distance between the metal and the pyrrole nitrogen atoms, and Δ_{Fe} is the displacement of the metal from the plane of the porphyrin ring.

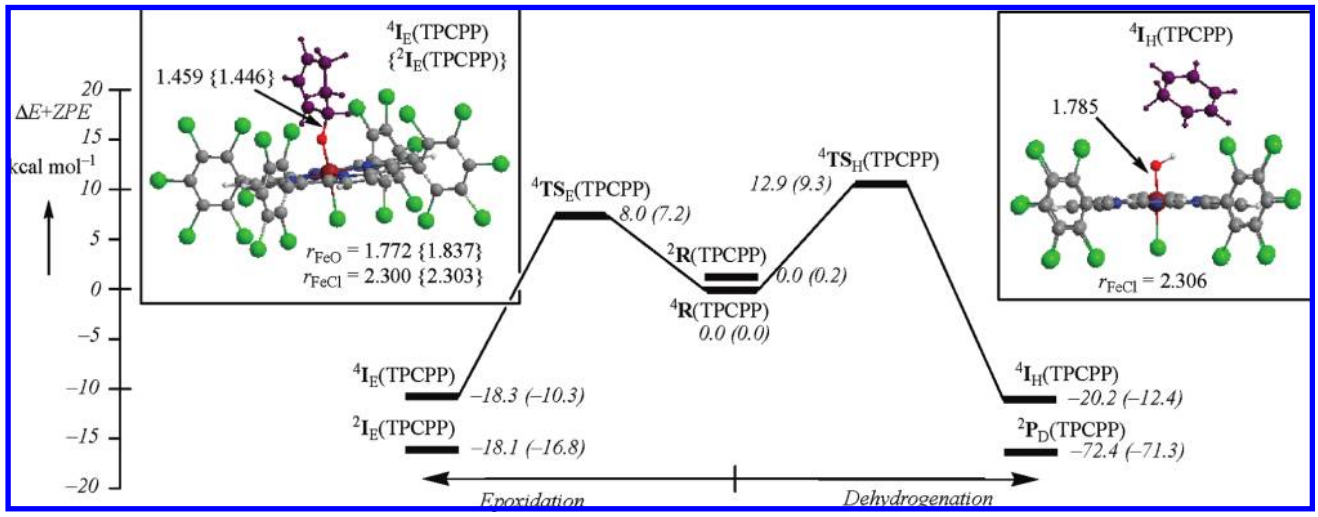

Figure 6. Potential energy profile of 1,3-cyclohexadiene epoxidation and dehydrogenation by ^{4,2}Cpd I(TPCPP), as calculated with UB3LYP. Energies are obtained with basis set B1, whereas values in parentheses are obtained with basis set B2 and solvent corrections. Also given are geometries of the intermediates along the epoxidation and dehydrogenation mechanism with bond lengths in angstroms and angles in degrees.

ZPE_{B1} level of theory, we find energies of −13.8, −13.7, −15.5, and −15.2 kcal mol^{-1} relative to isolated reactants for ^{4}**I**$_E$(TPP), ^{2}**I**$_E$(TPP), ^{4}**I**$_H$(TPP), and ^{2}**I**$_H$(TPP), respectively. These values are a few kilocalories per mole more exothermic than those observed for the unsubstituted porphyrin in Figure 3a. Moreover, the difference in energy between epoxidation and hydrogen abstraction intermediates is about 1.5 kcal mol^{-1} in favor of hydrogen abstraction, which is of the same order of magnitude as that observed for unsubstituted porphyrin. Therefore, the reaction exothermicity for formation of the intermediate complexes is close in energy for Cpd I(Por) and Cpd I(TPP), whereas the reaction is more exothermic for Cpd I(TPCPP). Therefore,

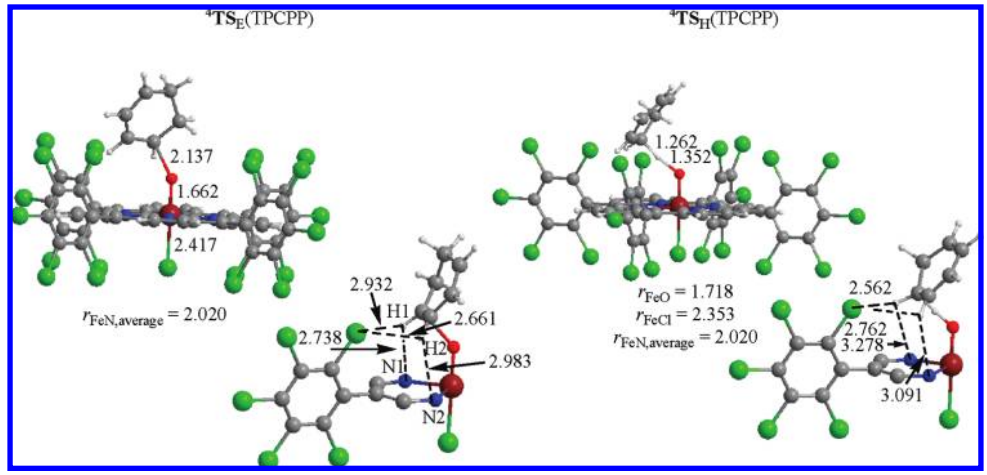

Figure 7. Optimized geometries of ^{4}**TS**$_E$(TPCPP) and ^{4}**TS**$_H$(TPCPP) with bond lengths in angstroms.

the halogen ligands of the meso-substituent influence the reaction mechanism by stabilizing the intermediate complexes of epoxidation. In the following, we will give a geometric explanation for this regioselectivity switch.

Optimized geometries of ^{4}**TS**$_E$(TPCPP) and ^{4}**TS**$_H$(TPCPP) are given in Figure 7. Geometrically, there are no dramatic differences between the structures in Figures 3 and 7. The Fe−Cl and Fe−O distances are slightly elongated for ^{4}**TS**$_E$(TPCPP) by about 0.05 Å. Moreover, the C−O bond in ^{4}**TS**$_E$(TPCPP) is enhanced by 0.026 Å with respect to ^{4}**TS**$_E$, whereas the O−H distance is shorter by 0.03 Å in ^{4}**TS**$_H$(TPCPP) compared with ^{4}**TS**$_H$. The main cause of destabilization of the hydrogen abstraction barrier, however, is due to the interactions of the substrate with the halogen ligands on the meso-substituents. Therefore, in the C−O activation barrier, the substrate approaches the oxo group with the double bond perpendicular to the C−O bond parallel to the porphyrin ring. As a consequence, the two hydrogen atoms attached to the carbon atoms of this double bond form hydrogen bonding interactions with the nitrogen atoms of the porphyrin ring as well as with a chloride atom of the $ArCl_5$ group. These hydrogen bond lengths are between 2.66 and 2.99 Å and will stabilize the structure in this conformation. In line with this, olefin epoxidation reactions by hydrogen peroxide in fluorinated alcohols were shown to be enhanced because of favorable interactions of the fluoride atoms through template-catalysis.[41] The hydrogen abstraction in ^{4}**TS**$_H$-(TPCPP) takes place with the substrate further away from the oxo group as compared with ^{4}**TS**$_H$ because the transferring hydrogen atom is located in between the substrate and the oxo group. As a result, the substrate is too far away to form favorable hydrogen bonding interactions with the porphyrin pyrrole nitrogen atom with CH−N distances well over 3 Å, and only hydrogen bonding occurs between C−H groups of the substrate with a chloride atom of the $ArCl_5$ ligand. Therefore, the hydrogen abstraction transition state is much less stabilized by polar interactions than the epoxidation transition state, and hence ^{4}**TS**$_E$(TPCPP) is considerably lower in energy than ^{4}**TS**$_H$-(TPCPP). Alternatively, the approach of the substrate to the oxo group from the top, that is, along the z axis or Fe−O axis, whereby the interactions between substrate and metal ligands are minimal, is not possible in heme systems because the electron transfer processes in the transition states favor a bent conformation for the Fe−O−substrate group.[42,43] The regioselectivity of epoxidation versus hydrogen atom abstraction by [Fe^{IV}=O(TPCPP$^{+\bullet}$)Cl], therefore, is determined by substrate binding to the oxidant, which favors the epoxidation mechanism.

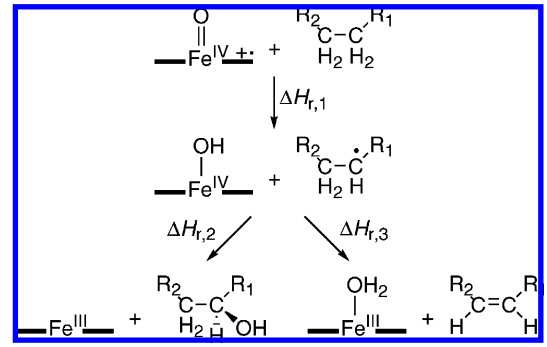

Figure 8. Mechanisms of hydrogen atom abstraction, hydroxylation, and dehydrogenation derived from DFT calculations.

Thermodynamic Factors That Determine Dehydrogenation versus Hydroxylation Regioselectivity. The cytochromes P450 generally react with substrates by hydrogen atom abstraction that leads to the formation of alcohol products, although occasionally, dehydrogenation reactions also occur. In the following, we will discuss factors that influence the regioselectivity of substrate dehydrogenation versus hydroxylation. Consider the overall reaction mechanism for both substrate dehydrogenation and hydroxylation in Figure 8. The reaction starts at the top with Cpd I and a molecule with two neighboring CH_2 groups and substituents R_1 and R_2 that determine whether the total molecule is an alkane or cycloalkane. The initial reaction is a hydrogen atom abstraction to form a hydroxo−iron(IV) complex and an alkyl radical with reaction enthalpy, $\Delta H_{r,1}$. It has been shown that this reaction enthalpy for the hydrogen atom abstraction is proportional to the difference in bond dissociation energy (BDE) between the C−H bond that is broken and the O−H bond that is formed in the process.[44] The BDE to split AH into A$^\bullet$ and a hydrogen atom is defined in eq 1. The energy to break the O−H bond in the hydroxo−iron(IV) complex is BDE_{FeOH}, and the energy to break the C−H bond in $R_2CH_2CH_2R_1$ is BDE_{CH2}. Combining these values of BDE_{FeOH} and BDE_{CH2} with $\Delta H_{r,1}$ gives eq 2.

$$AH \rightarrow A^\bullet + H^\bullet + BDE_{AH} \quad (1)$$

$$\Delta H_{r,1} = BDE_{CH_2} - BDE_{FeOH} \quad (2)$$

To make a prediction on regioselective substrate dehydrogenation versus hydroxylation, we calculated the C−H bond

TABLE 2: Calculated Bond Dissociation Energies and Reaction Energies for the Reactions Shown in Figure 8 from Isolated Species[a]

substrate	BDE_{CH_2}	$\Delta H_{r,1}$	BDE_{rad}	$\Delta H_{r,3}$	BDE_{COH}	$\Delta H_{r,2}$
ethane	96.2	9.5	36.7	−34.0	85.8	−55.5
trans-butane	92.6	5.9	33.5	−37.3	85.4	−55.2
cyclohexane	93.0	6.4	33.6	−37.2	85.8	−55.6
cyclohexene	77.7	−9.0	47.5	−23.3	69.1	−38.9
cyclohexadiene	69.0	−17.6	21.8	−49.0	59.7	−29.5

[a] All values are in kilocalories per mole.

strengths of several substrates, namely, ethane, *trans*-butane, cyclohexane, cyclohexene, and 1,3-cyclohexadiene. The calculated values of BDE_{CH_2} together with the value of BDE_{FeOH} = 86.6 kcal mol^{-1} from ref 17b give an estimate of the expected $\Delta H_{r,1}$ for hydrogen abstraction, and these data have been accumulated in Table 2. As follows, the hydrogen abstraction reaction is more exothermic with substrates with weak C−H bonds, and as a consequence, lower hydrogen abstraction barriers may also be expected. The reaction exothermicity of hydrogen abstraction from CHD is estimated to be −17.6 kcal mol^{-1} (Table 2). Using the same methods and basis sets, this value compares excellently with that calculated for the formation of $^4\mathbf{I}_H$ ($^2\mathbf{I}_H$) from isolated reactants where exothermicities of −18.2 (−18.2) kcal mol^{-1} were found in the gas phase.

The next step in the reaction mechanism is either hydroxyl rebound to the radical to form alcohol products with exothermicity, $\Delta H_{r,2}$, or a second hydrogen abstraction to form water and olefin with exothermicity, $\Delta H_{r,3}$. Analogous to eq 2 above, the latter reaction exothermicity ($\Delta H_{r,3}$) can be written as the difference in bond dissociation energy of the C−H bond of $R_2CH_2C^{\bullet}HR_1$ (designated BDE_{rad}) and the bond dissociation energy of the O−H bond in the water−iron(III) complex (designated BDE_{FeOH_2}), eq 3. A value of 70.8 kcal mol^{-1} for BDE_{FeOH_2} is calculated, whereas the values for BDE_{rad} and $\Delta H_{r,3}$ are given in Table 2. Saturated alkanes give very similar dehydrogenation reaction energies, but the most exothermic reaction is found for 1,3-cyclohexadiene, which is due to the increased resonance stabilization of product benzene.

$$\Delta H_{r,3} = BDE_{rad} - BDE_{FeOH_2} \quad (3)$$

The alternative reaction from the hydroxo−iron(IV) intermediate is substrate hydroxylation that involves hydroxyl rebound to the radical and formation of alcohol products via $\Delta H_{r,2}$. The bond dissociation energy to break the Fe−O bond in the hydroxo−iron(IV) complex (BDE_{FeOH}) is defined as in eq 4 and is calculated to be 30.2 kcal mol^{-1}.

$$Fe(IV)OH(Por)Cl \rightarrow Fe(III)(Por)Cl + OH^{\bullet} + BDE_{FeOH} \quad (4)$$

In a similar way, the hydroxyl affinities of the radical intermediates were estimated from the BDE_{COH} energies, as defined in eq 5.

$$AOH \rightarrow A^{\bullet} + OH^{\bullet} + BDE_{COH} \quad (5)$$

The reaction enthalpy for the hydroxylation reaction ($\Delta H_{r,2}$) is estimated using the values for BDE_{FeOH} and BDE_{COH}, and the results are given in Table 2. As follows, saturated alkanes have a large value of BDE_{COH}, and as a consequence, the hydroxylation rebound is highly exothermic. By contrast, the hydroxyl affinity of the radical obtained after hydrogen abstraction of CHD is very small (BDE_{COH} = 59.7 kcal mol^{-1}), which gives an overall hydroxylation rebound exothermicity of only $\Delta H_{r,2}$ = −29.5 kcal mol^{-1}. However, the competing dehydrogenation reaction is much more exothermic ($\Delta H_{r,3}$ = −49.0 kcal mol^{-1}), and hence a reaction of Cpd I with CHD gives dehydrogenated products rather than hydroxylated products. The other substrates given in Table 2 all have a more exothermic hydroxylation reaction as compared with the dehydrogenation reaction; therefore, these substrates will react with Cpd I to give hydroxylated products, except CHD, which has a lower energy dehydrogenation pathway because of the formation of the much more stable benzene product. Indeed, experimental studies on cyclohexene activation by a oxoiron(IV)porphyrin complex gave a mixture of epoxide and cyclohexenol products but no evidence of dehydrogenation.[45] The reaction exothermicities shown in Table 2, therefore, explain trends in product yields and explain the preference of substrate dehydrogenation by CHD.

Conclusions

Combined experimental and density functional studies of the reactions of cyclohexadiene with oxoiron(IV) porphyrin oxidants with variable meso-substituents are reported. It is shown that oxidants with electron-rich meso-substituents give benzene product, whereas electron-deficient meso-substituents react to form epoxide as a major product. Our DFT studies show that in the gas phase, the two processes are competitive with a small preference of hydrogen abstraction over epoxidation. However, a chemical system with pentachlorophenyl substituents (TPCPP) influences substrate binding and sterically hinders hydrogen atom abstraction, whereas the epoxidation transition state is stabilized. The present results give insight into the effect and influence of ligands on reaction mechanisms and regioselectivity of substrate monoxygenation by oxoiron(IV) porphyrins.

Acknowledgment. The research was supported by CPU time provided by the National Service of Computational Chemistry Software (NSCCS). Financial support from KOSEF/MEST through the CRI and WCU (R31-2008-000-10010-0) Programs is acknowledged. L.T. acknowledges the British Council for a Scholarship, and D.K. is a Ramanujan Fellow of the Department of Science and Technology (New Delhi).

Supporting Information Available: Cartesian coordinates of all structures described in this work and group spin densities and charges. This material is available free of charge via the Internet at http://pubs.acs.org.

References and Notes

(1) (a) Sono, M.; Roach, M. P.; Coulter, E. D.; Dawson, J. H. *Chem. Rev.* **1996**, *96*, 2841–2888. (b) Guengerich, F. P. *Chem. Res. Toxicol.* **2001**, *14*, 611–650. (c) Groves, J. T. *Proc. Natl. Acad. Sci. U.S.A.* **2003**, *100*, 3569–3574. (d) *Cytochrome P450: Structure, Mechanism, and Biochemistry*, 3rd ed.; Ortiz de Montellano, P. R., Ed.; Kluwer Academic/Plenum Publishers: New York, 2004. (e) Munro, A. W.; Girvan, H. M.; McLean, K. J. *Nat. Prod. Rep.* **2007**, *24*, 585–609.

(2) (a) van Eldik, R. *Coord. Chem. Rev.* **2007**, *251*, 1649–1662. (b) Makris, T. M.; von Koenig, K.; Schlichting, I.; Sligar, S. G. *J. Inorg. Biochem.* **2006**, *100*, 507–518. (c) Groves, J. T. *J. Inorg. Biochem.* **2006**, *100*, 434–447. (d) Woggon, W.-D. *Acc. Chem. Res.* **2005**, *38*, 127–136.

(3) Schlichting, I.; Berendzen, J.; Chu, K.; Stock, A. M.; Maves, S. A.; Benson, D. E.; Sweet, R. M.; Ringe, D.; Petsko, G. A.; Sligar, S. G. *Science* **2000**, *287*, 1615–1622.

(4) (a) Sligar, S. G.; Gunsalus, I. C. *Proc. Natl. Acad. Sci. U.S.A.* **1976**, *73*, 1078–1082. (b) Poulos, T. L. *Biochem. Biophys. Res. Commun.* **2003**, *312*, 35–39. (c) Kuznetsov, V. Y.; Poulos, T. L.; Sevrioukova, I. F.

Biochemistry **2006**, *45*, 11934–11944. (d) Purdy, M. M.; Koo, L. S.; Ortiz de Montellano, P. R.; Klinman, J. P. *Biochemistry* **2006**, *45*, 15793–15806. (e) Denisov, I. G.; Makris, T. M.; Sligar, S. G.; Schlichting, I. *Chem. Rev.* **2005**, *105*, 2253–2277.

(5) Poulos, T. L.; Finzel, B. C.; Howard, A. J. *J. Mol. Biol.* **1987**, *195*, 687–700.

(6) (a) Egawa, T.; Shimada, H.; Ishimura, Y. *Biochem. Biophys. Res. Commun.* **1994**, *201*, 1464–1469. (b) Kellner, D. G.; Hung, S. C.; Weiss, K. E.; Sligar, S. G. *J. Biol. Chem.* **2002**, *277*, 9641–9644. (c) Chiavarino, B.; Cipollini, R.; Crestoni, M. E.; Fornarini, S.; Lanucara, F.; Lapi, A. *J. Am. Chem. Soc.* **2008**, *130*, 3208–3217.

(7) Atkins, W. M.; Sligar, S. G. *J. Am. Chem. Soc.* **1987**, *109*, 3754–3760.

(8) (a) Hanzlik, R. P.; Hogberg, K.; Judson, C. M. *Biochemistry* **1984**, *23*, 3048–3055. (b) Hanzlik, R. P.; Hogberg, K.; Moon, J. B.; Judson, C. M. *J. Am. Chem. Soc.* **1985**, *107*, 7164–7167.

(9) (a) Dolphin, D.; Traylor, T. G.; Xie, L. Y. *Acc. Chem. Res.* **1997**, *30*, 251–259. (b) Nam, W. *Acc. Chem. Res.* **2007**, *40*, 522–531.

(10) Traylor, T. G.; Kim, C.; Richards, J. L.; Xu, F.; Perrin, C. L. *J. Am. Chem. Soc.* **1995**, *117*, 3468–3474.

(11) Fujii, H.; Kurahashi, T.; Tosha, T.; Yoshimura, T.; Kitagawa, T. *J. Inorg. Biochem.* **2006**, *100*, 533–541.

(12) (a) Wolak, M.; van Eldik, R. *Chem.—Eur. J.* **2007**, *13*, 4873–4883. (b) Hessenauer-Ilicheva, N.; Franke, A.; Meyer, D.; Woggon, W.-D.; van Eldik, R. *J. Am. Chem. Soc.* **2007**, *129*, 12473–12479. (c) Song, W. J.; Sun, Y. J.; Choi, S. K.; Nam, W. *Chem.—Eur. J.* **2006**, *12*, 130–137. (d) Nehru, K.; Seo, M. S.; Kim, J.; Nam, W. *Inorg. Chem.* **2007**, *46*, 293–298. (e) Park, M. J.; Lee, J.; Suh, Y.; Kim, J.; Nam, W. *J. Am. Chem. Soc.* **2006**, *128*, 2630–2634. (f) Song, W. J.; Seo, M. S.; DeBeer George, S.; Ohta, T.; Song, R.; Kang, M.-J.; Tosha, T.; Kitagawa, T.; Solomon, E. I.; Nam, W. *J. Am. Chem. Soc.* **2007**, *129*, 1268–1277.

(13) *Purification of Laboratory Chemicals*; Armarego, W. L. F., Perrin, D. D., Eds.; Pergamon Press: Oxford, U.K., 1997.

(14) (a) Traylor, T. G.; Miksztal, A. R. *J. Am. Chem. Soc.* **1987**, *109*, 2770–2774. (b) Bortolini, O.; Campestrini, S.; Di Furia, F.; Modena, G. *J. Org. Chem.* **1987**, *52*, 5093–5095.

(15) *Organic Syntheses*; Saltzman, H., Sharefkin, J. G., Eds.; Wiley: New York, 1973; Vol. *V*, p 658.

(16) La, T.; Miskelly, G. M.; Bau, R. *Inorg. Chem.* **1997**, *36*, 5321–5328.

(17) (a) de Visser, S. P. *J. Am. Chem. Soc.* **2006**, *128*, 9813–9824. (b) de Visser, S. P.; Tan, L. S. *J. Am. Chem. Soc.* **2008**, *130*, 12961–12974.

(18) de Visser, S. P. *Chem.—Eur. J.* **2006**, *12*, 8168–8177.

(19) (a) Becke, A. D. *J. Chem. Phys.* **1993**, *98*, 5648–5652. (b) Lee, C.; Yang, W.; Parr, R. G. *Phys. Rev. B* **1988**, *37*, 785–789.

(20) (a) Kumar, D.; de Visser, S. P.; Sharma, P. K.; Cohen, S.; Shaik, S. *J. Am. Chem. Soc.* **2004**, *126*, 1907–1920. (b) Kumar, D.; de Visser, S. P.; Shaik, S. *Chem.—Eur. J.* **2005**, *11*, 2825–2835. (c) de Visser, S. P.; Oh, K.; Han, A.-R.; Nam, W. *Inorg. Chem.* **2007**, *46*, 4632–4641. (d) Kim, S. J.; Latifi, R.; Kang, H. Y.; Nam, W.; de Visser, S. P. *Chem. Commun.* **2009**, 1562–1564.

(21) (a) Hay, P. J.; Wadt, W. R. *J. Chem. Phys.* **1985**, *82*, 270–283. (b) Hehre, W. J.; Ditchfield, R.; Pople, J. A. *J. Chem. Phys.* **1972**, *56*, 2257–2261.

(22) Frisch, M. J., Trucks, G. W.; Schlegel, H. B.; Scuseria, G. E.; Robb, M. A.; Cheeseman, J. R.; Montgomery, J. A., Jr.; Vreven, T.; Kudin, K. N.; Burant, J. C.; Millam, J. M.; Iyengar, S. S.; Tomasi, J.; Barone, V.; Mennucci, B.; Cossi, M.; Scalmani, G.; Rega N.; Petersson, G. A.; Nakatsuji, H.; Hada, M.; Ehara, M.; Toyota, K.; Fukuda, R.; Hasegawa, J.; Ishida, M.; Nakajima, T.; Honda, Y.; Kitao, O.; Nakai, N.; Klene, M.; Li, X.; Knox, J. E.; Hratchian, H. P.; Cross, J. B.; Adamo, C.; Jaramillo, J.; Gomperts, R.; Stratmann, R. E.; Yazyev, O.; Austin, A. J.; Cammi, R.; Pomelli, C.; Ochterski, J. W.; Ayala, P. Y.; Morokuma, K.; Voth, G. A.; Salvador, P.; Dannenberg, J. J.; Zakrzewski, V. G.; Dapprich, S.; Daniels, A. D.; Strain, M. C.; Farkas, O.; Malick, D. K.; Rabuck, A. D.; Raghavachari, K.; Foresman, J. B.; Ortiz, J. V.; Cui, Q.; Baboul, A. G.; Clifford, S.; Cioslowski, J.; Stefanov, B. B.; Liu, G.; Liashenko, A.; Piskorz, P.; Komaromi, I.; Martin, R. L.; Fox, D. J.; Keith, T.; Al-Laham, M. A.; Peng, C. Y.; Nanayakkara, A.; Challacombe, M.; Gill, P. M. W.; Johnson, B.; Chen, W.; Wong, M. W.; Gonzalez, C.; Pople, J. A. *Gaussian 03*, revision C.02; Gaussian, Inc.: Wallingford, CT, 2004.

(23) *Jaguar 7.0*; Schrödinger, LLC.: New York, 2007.

(24) (a) Hoe, W.-M.; Cohen, A.; Handy, N. C. *Chem. Phys. Lett.* **2001**, *341*, 319–328. (b) Perdew, J. P.; Burke, K.; Ernzerhof, M. *Phys. Rev. Lett.* **1996**, *77*, 3865–3868.

(25) (a) Perdew, J. P.; Chevary, J. A.; Vosko, S. H.; Jackson, K. A.; Pederson, M. R.; Singh, D. J.; Fiolhais, C. *Phys. Rev. B* **1992**, *46*, 6671–6687. (b) Becke, A. D. *J. Chem. Phys.* **1996**, *104*, 1040–1046.

(26) (a) Farinas, E. T.; Alcalde, M.; Arnold, F. *Tetrahedron* **2004**, *60*, 525–528. (b) Ruettinger, R. T.; Fulco, A. J. *J. Biol. Chem.* **1981**, *256*, 5728–5734.

(27) (a) Vaz, A. D. N.; McGinnity, D. F.; Coon, M. J. *Proc. Natl. Acad. Sci. U.S.A.* **1998**, *95*, 3555–3560. (b) Vaz, A. D. N.; Pernecky, S. J.; Raner, G. M.; Coon, M. J. *Proc. Natl. Acad. Sci. U.S.A.* **1996**, *93*, 4644–4648.

(28) Groves, J. T.; Gross, Z. In *Bioinorganic Chemistry: An Inorganic Perspective of Life*; Kessissoglon, D. P., Ed.; NATO Advanced Study Institute Series *459*; Kluwer Academic Publishers: Dordrecht, The Netherlands, 1995; pp 39−47.

(29) Song, W. J.; Ryu, Y. O.; Song, R.; Nam, W. *J. Biol. Inorg. Chem.* **2005**, *10*, 294–304.

(30) Takahashi, A.; Kurahashi, T.; Fujii, H. *Inorg. Chem.* **2007**, *46*, 6227–6229.

(31) Lim, M. H.; Jin, S. W.; Lee, Y. J.; Jhon, G. J.; Nam, W.; Kim, C. *Bull. Korean Chem. Soc.* **2001**, *22*, 93–96.

(32) Nam, W. In *Comprehensive Coordination Chemistry II*; Que, L., Jr., Tolman, W. B., Eds.; Elsevier: Oxford, U.K., 2003; Vol *8*, pp 281−307.

(33) (a) Ogliaro, F.; de Visser, S. P.; Groves, J. T.; Shaik, S. *Angew. Chem., Int. Ed.* **2001**, *40*, 2874–2878. (b) Schöneboom, J. C.; Neese, F.; Thiel, W. *J. Am. Chem. Soc.* **2005**, *127*, 5840–5853. (c) Groenhof, A. R.; Ehlers, A. W.; Lammertsma, K. *J. Am. Chem. Soc.* **2007**, *129*, 6204–6209. (d) Bathelt, C. M.; Zurek, J.; Mulholland, A. J.; Harvey, J. N. *J. Am. Chem. Soc.* **2005**, *127*, 12900–12908.

(34) Ghosh, A. *Acc. Chem. Res.* **1998**, *31*, 189–191.

(35) Green, M. T. *J. Am. Chem. Soc.* **1999**, *121*, 7939–7940.

(36) Shaik, S.; de Visser, S. P.; Ogliaro, F.; Schwarz, H.; Schröder, D. *Curr. Opin. Chem. Biol.* **2002**, *6*, 556–567.

(37) (a) de Visser, S. P.; Ogliaro, F.; Harris, N.; Shaik, S. *J. Am. Chem. Soc.* **2001**, *123*, 3037–3047. (b) de Visser, S. P.; Ogliaro, F.; Sharma, P. K.; Shaik, S. *J. Am. Chem. Soc.* **2002**, *124*, 11809–11826. (c) Kamachi, T.; Shiota, Y.; Ohta, T.; Yoshizawa, K. *Bull. Chem. Soc. Jpn.* **2003**, *76*, 721–732.

(38) Shaik, S.; Cohen, S.; de Visser, S. P.; Sharma, P. K.; Kumar, D.; Kozuch, S.; Ogliaro, F.; Danovich, D. *Eur. J. Inorg. Chem.* **2004**, 207–226.

(39) (a) Ogliaro, F.; Harris, N.; Cohen, S.; Filatov, M.; de Visser, S. P.; Shaik, S. *J. Am. Chem. Soc.* **2000**, *122*, 8977–8989. (b) Yoshizawa, K.; Kamachi, T.; Shiota, Y. *J. Am. Chem. Soc.* **2001**, *123*, 9806–9816. (c) Kamachi, T.; Yoshizawa, K. *J. Am. Chem. Soc.* **2003**, *125*, 4652–4661. (d) de Visser, S. P.; Kumar, D.; Cohen, S.; Shacham, R.; Shaik, S. *J. Am. Chem. Soc.* **2004**, *126*, 8362–8363. (e) Shaik, S.; Kumar, D.; de Visser, S. P. *J. Am. Chem. Soc.* **2008**, *130*, 10128–10140. (f) Balcells, D.; Raynaud, C.; Crabtree, R. H.; Eisenstein, O. *Chem. Commun.* **2008**, 744–746.

(40) Balding, P. R.; Porro, C. S.; McLean, K. J.; Sutcliffe, M. J.; Maréchal, J.-D.; Munro, A. W.; de Visser, S. P. *J. Phys. Chem. A* **2008**, *112*, 12911–12918.

(41) (a) de Visser, S. P.; Kaneti, J.; Neumann, R.; Shaik, S. *J. Org. Chem.* **2003**, *68*, 2903–2912. (b) Berkessel, A.; Adrio, J. A. *J. Am. Chem. Soc.* **2006**, *128*, 13412–13420.

(42) (a) Sharma, P. K.; de Visser, S. P.; Shaik, S. *J. Am. Chem. Soc.* **2003**, *125*, 8698–8699. (b) Kumar, D.; de Visser, S. P.; Sharma, P. K.; Hirao, H.; Shaik, S. *Biochemistry* **2005**, *44*, 8148–8158.

(43) de Visser, S. P. *J. Am. Chem. Soc.* **2006**, *128*, 15809–15818.

(44) Mayer, J. M. *Acc. Chem. Res.* **1998**, *31*, 441–450.

(45) Agarwala, A.; Bandyopadhyay, D. *Chem. Commun.* **2006**, 4823–4825.

JP9028694